Inverse of Low Resolution Line Halftone Images for Document Inspection

Biswajit Halder[1(✉)], Utpal Garain[2], Rajkumar Darbar[3], and Abhoy Ch. Mondal[1]

[1] Department of Computer Science, University of Burdwan, Bardhaman, West Bengal, India
biswajithalder88@gmail.com, abhoy_mondal@yahoo.co.in
[2] Indian Statistical Institute, Kolkata, India
utpal@isical.ac.in
[3] School of Information Technology, Indian Institute of Technology, Kharagpur, India
rajdarbar.r@gmail.com

Abstract. In this paper, a new inverse half toning method has been proposed for reconstructing low resolution line halftone images. This reconstruction is done in order to authenticate an image in question. The reconstructed image is compared with its original image in terms of standard image quality metrics such as peak signal to noise ratio (PSNR) and structural similarity index measure (SSIM). The existing inverse halftone methods have rarely considered line halftone images which are normally of low resolution and the quality of the inverse halftone largely depends on the characteristics like frequency or shape of halftone dots. Our proposed inverse halftone technique consists of two parts: at first, the resolution (in lines per inch, lpi) of an input image is estimated and a low level image from the binary line halftone image is constructed. In the second phase, gray level continuous image is generated from the low level description and the lpi information. The method is based on learning based pattern classification techniques namely, neural nets. A comparative study shows that the proposed method outperforms many existing inverse halftone techniques while dealing with line halftone images.

Keywords: Line half-tone · Inverse halftoning · RBF-NN · Image quality

1 Introduction

Halftone images are essential part of printed materials [1–3]. In printing pictures in books, a continuous tone original picture is first converted into a halftone (HT) one which finally gets printed in the book. Inverse halftone (IHT) is the method that attempts to generate the original picture from a given halftone image. IHT is important for several purposes. For instance, if we want to compare an original image with the one which has been actually printed by other printers. It may happen that the original copy of the image is not available at all and in this

U. Garain and F. Shafait (Eds.): IWCF 2012 and 2014, LNCS 8915, pp. 95–103, 2015.
DOI: 10.1007/978-3-319-20125-2_9

situation, IHT may help to regenerate the original picture from its HT image available in printed form. Reprinting of old books for which the original pictures are not available, IHT plays an important role. In today's world, IHT is an important tool for copyright authentication.

There are two types dots by which halftone images are composed of: (i) dispersed dot and (ii) clustered dot. Dispersed dots are of fixed size and dot diameter are not directly related to the dot frequency. The number of dots in a region defines the basis of tonal levels. The clustered dot occurs when the halftone dots are of variable sizes. In this scheme, the dot diameter is proportional to the dot frequency. Dispersed dots are used in limited case digital printing (e.g. laser jet printers, photocopiers, etc.) whereas clustered dots are used in large scale printing (e.g. offset printing, lithography, silkscreen printing, etc.)

In literature, various types of IHT techniques are available [4,5]. Almost all of these techniques considered dispersed dot halftone images which are largely relevant for digitally printed materials. The effectiveness of these methods for clustered dot halftone images is not well studied. Some works have reported results on both dispersed as well as clustered dots where dealing with dispersed dots is mostly stressed upon. This dominant trend, i.e. dealing with the dispersed dots as observed in the existing IHT methods maybe because of the easy availability of digital printers under lab environment. Original pictures are converted into corresponding their halftone versions which are then printed using digital printers. As the digital printers are used, dispersed dots came into discussion. However, for large scale printing offset/silk screen printers instead of digital ones are used. Therefore, IHT methods working on clustered dots are important in many practical situations. Moreover, dispersed dot halftone images are generally of higher resolution (around 150 lines per inch or lpi and more) than that of clustered dot based halftone images (as low as 50 lpi to as high as 150 lpi). Consequently, efficiency of most of the existing IHT methods on low resolution halftone images is also not well explored. This paper attempts to fill this gap by considering design of an efficient IHT method working on clustered dot halftone images.

The clustered dots can be of different shapes. The line halftone dots are one of them and mostly used by the printing houses. Line half tone images are commonly used in printed books, old manuscripts, magazines etc. including many security documents like certificates, bank checks, currency notes, legal deeds and so on. In security documents, line halftone images are normally used as background design that serves as a protection against counterfeiting. Such design involves micro print-line patterns, guilloches patterns, latent image pattern, relief line pattern etc. Most of these patterns are produced from continuous tone image. The design details of such patterns are not clear with the naked eye but become clear with magnification. Characteristics of these line patterns are line thickness, line density and ink colour. Fine-line design features are changed in the event of a photocopying attack. For example, when a forger attempts to copy the page, the design will appear blurred and display a pattern spread. Generally, a document examiner inspects this deformation with a magnifier [6–8]. The document in question is inspected using different light sources, i.e. transmitted light, oblique light, etc. This inspection is grossly manual and therefore, time consuming. For quick decision-making and for better visual inspection, a sophisticated machine-assisted technique is called for. This paper is aimed at developing an inverse half toning technique (IHT) for authenticating line HT images. The method attempts to formulate a statistical measure in order to judge the quality of the image in question against the original image. We have considered line halftone image at three different resolutions namely, 60, 70, and 80 lpi which are commonly used in practice.

Another significant contribution of this study is to use learning based pattern classification technique for designing the IHT method. The existing methods rarely exploit this technique rather make use of static template or edge analysis based pattern matching. Many techniques borrow idea from digital signal processing. Pattern classification based inverse halftoning has also been attempted in few works [9,10]. These methods do not consider resolution of an input image separately and therefore, inverse halftoning is done based on a overall learning over images of many resolutions. Our method brings novelty by finding the lpi information so that generation of inverse halftone becomes more precise. Secondly, empirically we observe that use of more than one neural net gives better quality inverse halftone than the one given by only one neural net. First neural net generates an approximate low level image (k-level, where $2 < k < 256$) which is taken by the second neural net as input and produces the final gray tone image. Lastly, we have presented a comparative study to show the effectiveness of our proposed method over several existing IHT methods when applied on line halftone images.

2 The Proposed Inverse Transform Method

The main of the inverse transform method is to take a line halftone (HT) image as input and produce a high quality gray-scale image corresponding to the input. A radial basis function neural net (RBF-NN) is the core of this transform method. The reason for using RBF-NN as the neural network lies in the fact that the inverse transform is a complex non-linear process and for doing this, RBF-NN shows better performance for universal non-linear approximation over the other neural nets (e.g. MLP-NN) [9].

The reconstruction function is given by

$$C = \sum_{h}^{n} w_h \cdot \phi(||x - t_h||) + B \tag{1}$$

where n is the total number of input samples applied for output neuron C which corresponds to the intensity level of a pixel $(i,\, j)$ in the output image, w_h is the synaptic weight connecting hidden neuron h to output neuron, B is a bias of the output neuron and the activation function $\phi(\cdot)$ is defined as

$$\phi(||x - t_h||) = \exp\left\{\frac{-(||x - t_h||^2}{2\sigma_h^2}\right\} \tag{2}$$

where the set of centres $\{t_h | h = 1, 2, \ldots, n\}$ are m^2-dimensional vectors to be determined, x is the m^2 dimensional pattern obtained by placing a $m \times m$ template around the (i, j) pixel of the input image, and σ_h is the variance of Gaussian function. The gradient descent is used for error-correction learning process.

Two different architectures are used to achieve this transform.

Architecture 1. A single RBF-NN is used that takes the binary HT image as input, predicts lpi of the input image and generates the gray image as output. This is somewhat similar to what has been used in previous works for inverse halftoning of dithered halftone images [9], but these works do not compute lpi information.

Architecture 2. This architecture consists of two levels of RBF-NNs as shown in Fig. 1. The first level takes the input image, I_{HT} and predicts the lpi information for the given image. In addition, the first level produces a low level (k-level) image, I_k. The lpi information helps to choose a particular NN on the second level. If we consider three different lpi based HT images (I_{HT}) then three different RBF-NNs corresponding to three specific lpi values are present on the second level. Depending upon the lpi detected by the first level RBF-NN, the intermediate k-level image (I_k) is passed to the particular RBF-NN on the second level. The RBF-NN of the second level produces the final gray scale image (I_G).

The values of m and k have definite impact on the quality of the inverse halftone and therefore, several alternatives have been tried. In our experiment, three different values of m namely, 3, 5 and 7 and three different values for k namely, 4, 8 and 16 are used. Variation in m will give different pixel templates based on which prediction of lpi information and the intensity level of a pixel in the output image is predicted. Variation in k defines the intermediate approximated image at different intensity levels.

3 Experimental Protocol

3.1 Dataset

In this experiment, five standard digital grayscale images namely, (i) *Peppers*, (ii) *Mandrill*, (iii) *Barbara*, (iv) *Atlas hand* and (v) *Lena eye* which have no background have been considered. Line HT images are generated using a commercial software namely Adobe Photoshop Software 7.0. All the images are processed at 100 dpi resolutions with specified screen angle namely, 45° and dot frequencies of 60, 70 and 80 lpi. Printing is done through single color offset printing machine (black ink used here). Printed images are digitized by flatbed HP scanner (ScanJet 8250) with same resolution (i.e. 100 dpi). Binary images are obtained by using Otsu thresholding method.

HT binary images of the first three images (i.e. *Peppers*, *Mandrill* and *Barbara*) have been considered for training the RBF-NNs and remaining two images (i.e. *Lena eye* and *Atlas hand*) have been considered for testing. For architecture-1, i.e. use of only one RBF-NN, about 500,000 (500K) binary

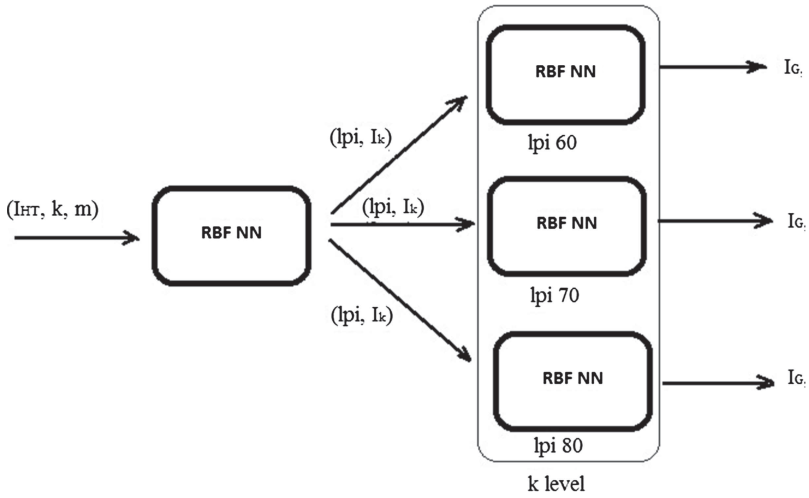

Fig. 1. Block diagram of Architecture 2

feature vectors tagged with lpi information and gray value are generated from the training halftone images. For architecture-2, i.e., two-level RBF-NN, the first-level RBF-NN is trained with feature vectors tagged with lpi, k-level value and gray level. The k-level values are generated by down-sampling the original gray images. The gray level tag is not required by the first-level RBF-NN, but it is used by the second RBF-NN.

3.2 Evaluation Strategy

Two methods namely, peak-signal-to-noise ratio (PSNR)and structural similarity index measure (SSIM) [11] often used for measuring image quality are applied for judging the efficiency of the proposed inverse halftoning method as well as comparing its performance with some of the well cited previous studies. PSNR value is inversely proportional with the mean square error (MSE). The value of SSIM is computed combining correlation, luminance and contrast. Its range lies in $[0, 1]$. If SSIM be 1 then both images are maximally correlated.

3.3 Results and Discussions

The performance of the inverse transform methods are presented on two pictures namely *Atlas hand* and *Lena eye* which are halftoned at three different resolutions: 60, 70 and 80 lpi. The performance of the architecture-1 is presented first in Table 1.

Note that for the *Atlas hand* PSNR values of around 27-28 and SSIM value of around 0.8 is achieved which is slightly better than what is obtained by the same architecture but without using lpi information [9]. Without using lpi information

Table 1. Performance of a single RBF-NN based Inverse Transform Method (Architecture-1)

Image	LPI	Context Pattern ($m \times m$)					
		3×3		5×5		7×7	
		PSNR	SSIM	PSNR	SSIM	PSNR	SSIM
Atlas hand	60	25.052	0.859	***27.805***	***0.901***	27.200	0.891
	70	24.868	0.873	***27.283***	***0.896***	27.240	0.890
	80	18.010	0.710	27.010	0.789	***28.040***	***0.810***
Lena eye	60	21.673	0.565	18.273	0.505	***21.797***	***0.571***
	70	21.585	0.557	***23.903***	***0.641***	23.660	0.636
	80	20.735	0.514	***23.956***	***0.624***	23.656	0.623

(i.e. if the training of the neural is done without lpi information) PSNR value of around 24-25 is obtained. The same trend is supported by the *Lena eye* image. This shows lpi information better guides the inverse halftoning process. Context pattern based on which features are extracted around a pixel has definite effect and the result shows that 5×5 context produces best average case result. We can further note that similar inverse halftoning methods [9,10] produced image giving PSNR of around 30-31 when the halftones are based on dispersed dots and printed digitally. The reason is the resolution which is far more (around 150 lpi) for dispersed dot based halftones than it is in line halftones.

Next the performance of the two-stage RBF-NN is reported in Table 2. Here a k-level is approximated image is generated first which is then converted into gray tone. Quality of inverse halftone image has been investigated at different values of k. It is to be noted that for all cases, this 2-level RBF-NN architecture gives better performance than single RBF-NN. Though the amount of improvement looks small in terms of PSNR and SSIM values but these improvements are statistically significant for all the three resolutions, $p < 0.05$ by a two-tail t-test. Figures 2 and 3 show the inverse halftone images at different resolution levels. Results for 5×5 context pattern are shown in these figures.

From the Tables 1 and 2, one more observation maybe noted. In these tables, SSIM values varies from 0.5 to 0.9 whereas PSNR varies from 18 to 29 (dB). It is observed that when SSIM increases from 0.2 to 0.8, PSNR increases linearly or nearly following a straight line. However, when SSIM rises to 0.8 or higher, PSNR increases rapidly. This observation is supported by the findings in [11].

Next, we compare the performance of our method against the largely cited inverse halftoning methods [12–15] which have been shown performing well on dispersed halftone images. We checked their performance on line halftone images and results are reported in Table 3. The comparison shows that the proposed method outperforms the other methods often by significant margin based on both the metrics, i.e., PSNR and SSIM and for all the three resolutions.

Table 2. Performance of two-stage RBF-NN based Inverse Transform Method (Architecture-2)

Image	LPI	k	Context Pattern ($m \times m$)					
			3×3		5×5		7×7	
			PSNR	SSIM	PSNR	SSIM	PSNR	SSIM
Atlas hand	60	4	24.875	0.866	27.553	0.899	27.400	0.896
		8	25.526	0.877	27.812	0.890	***27.900***	***0.903***
		16	24.874	0.873	27.843	0.901	27.700	0.893
	70	4	24.884	0.870	26.778	0.889	28.705	0.891
		8	25.005	0.870	26.870	0.879	27.690	0.876
		16	24.936	0.873	27.071	0.893	***29.670***	***0.909***
	80	4	18.370	0.750	27.572	0.809	28.670	0.887
		8	18.887	0.768	27.670	0.890	***28.900***	***0.894***
		16	18.910	0.784	27.550	0.886	28.400	0.865
Lena eye	60	4	21.108	0.528	23.188	0.610	23.437	0.597
		8	22.875	0.582	23.753	0.613	***24.387***	0.622
		16	22.295	0.588	24.026	***0.631***	23.921	0.619
	70	4	21.021	0.521	23.514	0.615	24.893	0.688
		8	22.388	0.578	23.798	0.625	***26.368***	***0.807***
		16	22.972	0.598	24.145	0.644	24.184	0.642
	80	4	21.219	0.518	23.735	0.601	23.904	0.616
		8	22.060	0.561	25.050	0.623	***25.066***	***0.682***
		16	22.590	0.573	24.046	0.619	24.289	0.634

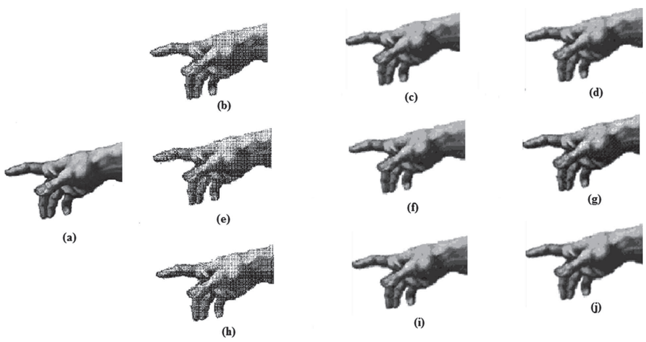

Fig. 2. Inverse Halftoning of *Atlas hand*: (a) original gray image, (b), (e), (h): line halftone document images at 60, 70 and 80 lpi; (c), (f), (i): inverse halftone images at 60, 70, 80 lpi by using single RBF-NN architecture-1; (d), (g), (j): inverse halftone images at 60, 70, 80 lpi by using two-stage RBF-NN architecture-2.

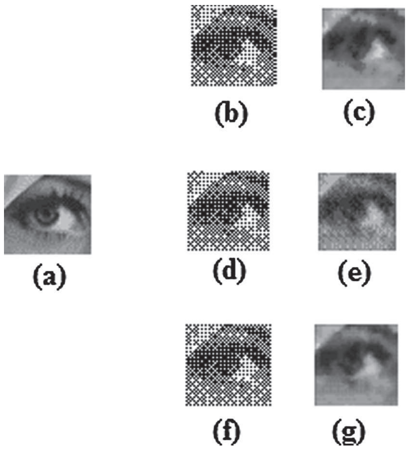

Fig. 3. Inverse Halftoning of *Lena eye*: (a) original gray image, (b), (d), (f): line halftone document images at 60, 70 and 80 lpi; (c), (e), (g): inverse halftone images at 60, 70, 80 lpi by using two-stage RBF-NN architecture-2.

Table 3. Performance Comparison: the first row for each method corresponds to the image *Atlas hand* and the second corresponds to the image *Lena eye*

IHT Method	60 LPI		70 LPI		80 LPI	
	PSNR	SSIM	PSNR	SSIM	PSNR	SSIM
LPA-ICI [12]	25.502	0.782	26.005	0.845	26.001	0.845
	24.190	0.631	24.364	0.650	24.232	0.636
WInHD [13]	25.589	0.862	25.596	0.862	25.592	0.862
	24.306	0.655	24.722	0.687	24.370	0.657
MAP [14]	26.996	0.892	26.999	0.892	26.995	0.892
	24.136	0.621	24.455	0.634	24.170	0.617
LUT [15]	24.885	0.780	25.213	0.781	25.211	0.780
	23.341	0.621	23.806	0.630	23.428	0.624
Our Method	27.900	0.903	29.670	0.909	28.900	0.894
	24.387	0.631	26.368	0.857	25.066	0.682

4 Conclusion

Though line halftone technique is largely used in practice for large scale printing but there was little research on inverse halftoning of line halftone images. This study presents a neural net based inverse halftoning method for line halftones. Experimental results show that the proposed method works well for the line halftones compared to the several existing methods. As line halftones are generally of low resolution images, inverse halftone images give slightly less PSNR and SSIM value compared to the those obtained for dispersed dot (higher resolution) based halftones. The present study can be extended in several directions. At first, improvement of inverse halftone images is definitely an area where more research is needed. It is shown here that a two-stage neural net performs better than a single stage architecture. This can be further extended to investigate whether a series of neural net could produce better quality inverse halftone.

As the current work is motivated by the practical need of generating original gray tone image in situation where the original image is not available or the printed halftone is in question of copyrighting issue, performance evaluation on a much larger dataset is required to bring out the potential of the present approach in practical scenario. Once established its efficiency on a larger dataset the present method could of good assistance for the forensic scientists, printing engineers and even for restoration of many historical documents.

References

1. Lau, D.L., Arce, G.R.: Modern Digital Halftoning. Marcel Dekker, New York (2001)
2. Knuth, D.E.: Digital halftones by dot diffusion. Published ACM Trans. Graph. (TOG) **6**(4), 245–273 (1987)
3. Analoui, M., Allebach, J.P.: Model based halftoning using direct binary search In: Proceedings SPIE Human Vision, Visual Digital Display III, vol. 1666, pp. 96–108, San Jose, CA (1992)
4. Kite, T.D., Damera-Venkata, N., Evans, B.L., Bovik, A.C.: A fast, high-quality inverse halftoning algorithm for error diffused halftones. IEEE Trans. Image Process. **9**(9), 1583–1592 (2000)
5. Chung, K.L., Wu, S.T.: Inverse halftoning algorithm using edge-based lookup table approach. IEEE Trans. Image Process. **14**(10), 1583–1589 (2005)
6. Reserve Bank of India, High Level RBI Group Suggests Steps to Check Menace of Fake Notes, Press release: 2009–2010/232 (2009)
7. Procedure Manuals, prepared by Directorate of Forensic Science, Ministry of Home Affairs, Government of India. http://www.dfs.gov.in
8. Counterfeit Banknotes, report of the parliamentary office of science and technology, UK (1996). www.parliament.uk/briefing-papers/POST-PN-77.pdf
9. Huang, W.B., Su, A.W.Y., Kuo, Y.H.: Neural network based method for image halftoning and inverse halftoning. Expert Syst. Appl. **34**(4), 2491–2501 (2008)
10. Chang, P.C., Yu, C.S.: Neural net classification and LMS reconstruction to halftone images. In: Proceedings SPIE Visual Communications and Image Processing, vol. 3309, pp. 592–602 (1998)
11. Hore, A., Ziou, D.: Image quality metrics: PSNR vs. SSIM. In: Proceedings IEEE International Conference of Pattern Recognition, pp. 2366–2369 (2010)
12. Foi, A., Katkovnik, V., Egiazarian, K., Astola, J.: Inverse halftoning based on the anisotropic LPA-ICI deconvolution. In: Proceedings of the International TICSP Workshop Spectral Method Multirate Signal Processing (SMMSP), pp. 49-56, Vienna (2004)
13. Neelamani, R., Nowak, R., Baraniuk, R.: WInHD: wavelet-based inverse halftoning via deconvolution. IEEE Trans. Image Proc. **6**(12), 1673–1687 (2002)
14. Stevenson, R.: Inverse halftoning via MAP estimation. IEEE Trans. Image Proc. **6**, 574–583 (1997)
15. Mese, M., Vaidyanathan, P.P.: Look-up table (LUT) method for inverse halftoning. IEEE Trans. Image Proc. **10**(10), 1566–1578 (2001)